Electronic states in the t–J model near magnetic phase transitions

Yu. A. Izyumov, B. M. Letfulov, and E. V. Shipitsyn

Institute of the Physics of Metals, Ural Branch of the Russian Academy of Sciences, 620219 Ekaterinburg, Russia

We use the generalized random phase approximation (GRPA), suggested earlier by us for calculating the dynamic magnetic susceptibility, to study the electronic states in the paramagnetic phase within the t–J model. We calculate the electron Green's function defined via the Hubbard X-operators and show that its self-energy and terminal parts are expressed in terms of the dynamic magnetic and dielectric susceptibilities. We show that near a ferromagnetic or antiferromagnetic phase transition point the contribution from quasistatic fluctuations dominates. Allowing for this contribution leads to the Green's function becoming incoherent, which means that the system undergoes a crossover from the Fermi-liquid behavior to that of strong electron correlations. This occurs at a concentration near the critical value n_c, at which there also occurs a crossover from a purely collectivized magnetism to one with localized magnetic moments. The extent to which the electronic states are of a nonquasiparticle nature increases near magnetic phase transitions. We calculate the Curie and Néel temperatures T_C and T_N over a broad range of electron concentrations. We also show that T_N decreases sharply near a half-filled state as the hole concentration grows and that antiferromagnetism vanishes at a certain concentration. Outside the antiferromagnetism region the magnetic correlation length decreases in inverse proportion to the square root of hole concentration and is weakly temperature dependent. Thus, we show that the magnetic behavior of the t–J model near a half-filled state qualitatively resembles the behavior of high-T_c copper-oxide superconductors.

1. INTRODUCTION

In recent years there has been extensive research in the field of the t–J model, which is one of the main models in the theory of strongly correlated systems. The model assumes that electrons travel in the lattice by hopping from one site to a neighboring site (with the transition matrix element t), provided that each site can carry no more than one electron. At the same time the electrons at neighboring sites interact via exchange forces, characterized by the exchange integral J of the antiferromagnetic sign. This model can be interpreted as the limiting case of the Hubbard model when the single-site Coulomb repulsion is large, $U \gg t$. Then, after states with two electrons at a site are excluded, there emerges a strongly correlated electron system with an indirect exchange interaction $J = t^2/U$, with $J \ll t$. It is in this sense that we interpret the t–J model, although there exists a broader interpretation as the fundamental model of strongly correlated systems with two independent parameters, t and J.

It is assumed[1] that the t–J model with $J \ll t$ is the basic model for describing the electronic structure of copper-oxide high-T_c superconductors. Hence, the main interest lies in studying this model in two-dimensions world and close to the situation of a half-filled band, that is, for an electron concentration $n = 1$, where n is the number of electrons per lattice site. The literature devoted to a thorough examination of the t–J model is vast. The interested reader can turn to Ref. 2 for a review.

If our interest is not restricted to high-T_c supercon-ductors, there emerges a general problem of studying the behavior of the t–J model within a broad interval of electron concentrations $0 < n < 1$. One of the main questions then is, at what concentrations does the electron system lose the properties of a Fermi liquid and go over to a strong-correlations mode? In Refs 3–6 we developed the generalized random phase approximation (GRPA) for the t–J model, similar to the random phase approximation (RPA) for the ordinary Fermi liquid, which enables studying the properties of the t–J model for arbitrary electron concentrations. It was found that near a certain critical concentration $n_c = \frac{1}{2}$ there is a crossover in the magnetic behavior of the system from purely collectivized magnetism to magnetism with localized magnetic moments. For one thing, the magnetic susceptibility for $n > n_c$ contains two contributions: of the Pauli type, weakly depended on the temperature T, and of the Curie type, proportional to T^{-1}. The latter indicates that localized magnetic moments have developed in the system.

Note that describing the emergence of localized moments in an ordinary Fermi liquid is extremely complicated. To tackle this problem many approaches have been used: the self-consistent spin-fluctuation theory,[7] the functional integration method,[8] and the ordinary diagrammatic technique for Fermi systems with the small parameter $U/t \ll 1$ (see Ref. 9). In the t–J model the inverse parameter is small, $t/U \ll 1$, and to effectively use this parameter it is convenient to employ the perturbation theory in the form of the diagrammatic technique with X-operators, first

1063-7761/94/050731-12$10.00

formulated for the complete Hubbard model[10] and then for the t–J model.[3] In terms of this technique, the GRPA consists in summing all loop diagrams with electron Green lines, which describe a strongly correlated system in the "Hubbard-I" approximation,[11] similar to RPA for an ordinary Fermi liquid, which consists in summing all electron loops with free-particle Green's functions.[12]

The Hubbard-I approximation allows only for the narrowing of the electron band due to electron correlations, while the states themselves are of a propagator nature, that is, do not fade out. Here the variation of electron concentration from 0 to 1 inflicts no radical changes in the electron spectrum even when the condition $n > n_c$ with localized magnetic moments is reached. The GRPA provided a method stepping outside the boundaries of this approximation; we used it in Ref. 3 to study the magnetic behavior of the system. We began our study of electronic states with the GRPA in Ref. 6, where we arrived at general diagrammatic expressions for electron Green's functions and calculated the GRPA- correction in these functions. But these results were of a preliminary nature, since in Ref. 6 we considered only the limiting case $U \to \infty$ and allowed for fluctuations of only transverse components of spin, while the fluctuations of the longitudinal components of spin and charge fluctuations were ignored. Nevertheless, we established a fairly general structure of the electron Green's functions and showed that with strongly correlated systems it is highly important to allow for corrections in the numerator of such a function, which leads to renormalization of the spectral density. These corrections always emerge in the diagrammatic technique for operators whose commutator is not an c-number (such a situation occurs for spin operators and X-operators) and correspond to what is known as terminal parts of diagrams.[13]

In this paper we calculate the electron Green's function of the t–J model in the GRPA. We find that the self-energy and terminal parts are expressed in terms of the dynamical magnetic and dielectric susceptibility and describe the interaction of electrons with spin and charge fluctuations. We study in detail the system's behavior near a magnetic phase transition to a ferromagnetic or antiferromagnetic structure, when long-wave quasistatic fluctuations are important. In this situation the DC contribution to the magnetic susceptibility of the Curie–Weiss type dominates. Since this contribution exists only for $n > n_c$, it is clear that as the point n_c is passed, the processes of elastic scattering on static fluctuations of the Ornstein–Zernike type are incorporated fairly rapidly. This is the reason for the incoherent nature of the electronic states. Thus, in the neighborhood of the critical concentration n_c the system crosses over from the Fermi-liquid mode to the mode of strong electron correlations, where the electronic states do not represent quasiparticles. The scattering of electrons on dynamic fluctuations does not change its nature as the point n_c is passed, with the result that the electron contribution, which varies monotonically with n, in the first approximation can be dropped. The closer to the line of the magnetic phase transition we are the more exact such an approach is.

Since in the GRPA the magnetic susceptibility is determined by the loop diagrams constructed from electron Green lines, there is the problem of finding in a self-consistent manner the corrections to these loops caused by the scattering of electrons on quasistatic fluctuations. This problem as well is solved in this paper.

We begin with a brief discussion of the main principles of the diagrammatic technique for the t–J model and the formulation of the GRPA, which although discussed in Ref. 3 are required here to calculate the electron Green's function. Although the diagrammatic equations may seem cumbersome, the analytical results obtained with their help are fairly neat and physically obvious.

2. THE t–J MODEL IN TERMS OF THE HUBBARD OPERATORS

So as not to explicitly take into account the conditions that exclude the possibility of two electrons appearing at the same site, it is convenient to represent the Hamiltonian of the t–J model in terms of Hubbard operators:[3]

$$\mathcal{H} = \mathcal{H}_0 + \mathcal{H}_{kin} + \mathcal{H}_{eff},$$

where

$$\mathcal{H}_0 = \varepsilon_+ \sum_i X_i^{++} + \varepsilon_- \sum_i X_i^{--}, \tag{2.1}$$

$$\mathcal{H}_{kin} = t \sum_{ij} \sum_\sigma X_i^{\sigma 0} X_j^{0\sigma}, \tag{2.2}$$

$$\mathcal{H}_{eff} = J \sum_{ij} (X_i^{-+} X_j^{+-} - X_i^{++} X_j^{--}) \tag{2.3}$$

is the single-site, kinetic, and exchange–correlation energies, respectively. Here $\varepsilon_\sigma = -\frac{1}{2}\sigma h - \mu$ is the energy of the state of a single electron at a site with spin $\sigma = +,-$ in a magnetic field ($h = g\mu_B H$, with H the magnetic field strength). The summation in (2.2) and (2.3) is over nearest neighbors.

It is clear that the Hamiltonian of the t–J model is expressed in terms of eight X-operators, four of which ($X_i^{\sigma 0}$ and $X_j^{0\sigma}$) are Fermi-like, two (X_i^{+-} and X_i^{-+}) Bose-like, and the remaining two (X_i^{++} and X_i^{--}) diagonal. We define the Matsubara Green's functions on these operators:

$$\mathcal{G}_\sigma(i\tau; j\tau') = -\langle T X_i^{0\sigma}(\tau) X_j^{\sigma 0}(\tau') \rangle,$$

$$D_\perp(i\tau; j\tau') = -\langle T X_i^{+-}(\tau) X_j^{-+}(\tau') \rangle,$$

$$D_\parallel(i\tau; j\tau') = -\langle T M_i(\tau) M_j(\tau') \rangle, \tag{2.4}$$

$$D_c(i\tau; j\tau') = -\langle T N_i(\tau) N_j(\tau') \rangle,$$

where $M_i = X_i^{++} - X_i^{--}$, and $N_i = X_i^{++} + X_i^-$. Here $\mathcal{G}_\sigma$ describes the propagation of electrons, $D_\perp$ and $D_\parallel$ are the Green's functions of the transverse and longitudinal spin components, and D_c is the density–density Green's function. All notation is standard.[14]

We discussed the perturbation theory with the Hamiltonian $\mathcal{H}_{int} = \mathcal{H}_{kin} + \mathcal{H}_{eff}$ in detail in Refs. 3 and 6, so that

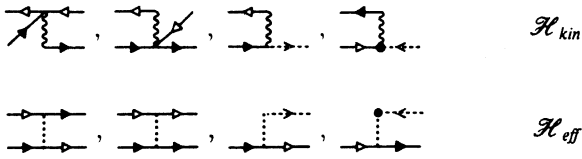FIG. 1. Elementary vertex parts for the interactions $\mathscr{H}_{\text{kin}}$ and $\mathscr{H}_{\text{eff}}$.

here we give only the main elements of the diagrammatic technique, the Green lines and the "interaction" lines:

$$G_{\uparrow}^{0} = \text{—▶—}, \quad G_{\downarrow}^{0} = \text{—▶—}, \quad D^{0} = \text{··▶··}.$$

$$\varepsilon(\mathbf{k}) = \text{\large www}, \quad J(\mathbf{k}) = \text{······}. \tag{2.5}$$

Here

$$\varepsilon(\mathbf{k}) = t \sum_{\Delta} e^{i\mathbf{k}\Delta}, \quad J(\mathbf{k}) = J \sum_{\Delta} e^{i\mathbf{k}\Delta}, \tag{2.6}$$

and G_{σ}^{0} and D^{0} are the Fermi and Bose Green's functions,

$$G_{\sigma}^{0}(i\omega_{n}) = \frac{1}{i\omega_{n} - \varepsilon_{\sigma}}, \quad D^{0}(i\omega_{n}) = \frac{1}{i\omega_{n} - h}, \tag{2.7}$$

with odd and even discrete frequencies. Summing the simplest diagram series,[10] we go from single-site fermion Green's functions to the propagator Green's function:

$$G_{\sigma}^{0}(k) = \frac{1}{i\omega_{n} - \langle F^{\sigma 0} \rangle \varepsilon(\mathbf{k}) - \varepsilon_{\sigma}}, \tag{2.8}$$

where $k = (\mathbf{k}, i\omega_{n})$ is the four-momentum, and $\langle F^{\sigma 0} \rangle \varepsilon(\mathbf{k})$ is the electron energy in the lower Hubbard subband; $F^{\sigma 0} = X^{00} + X^{\sigma\sigma}$. In the literature this approximation is known as the Hubbard-Iapproximation.[1] In what follows we assume that all the electron Green lines correspond to the propagator functions (2.8).

The terms $\mathscr{H}_{\text{kin}}$ and $\mathscr{H}_{\text{eff}}$ in the Hamiltonian generate the elementary vertex parts as depicted in Fig. 1. They describe electron–electron scattering and processes of emission and absorption of a single magnon. Generally speaking, there are also vertices involving two or more magnons,[3] but these are not considered here.

Note that at all vertices containing no outgoing lines there is a cumulant. This is a feature of the diagrammatic technique for operators whose commutators are not c-numbers. Another common feature is the existence of vertices with three (fermion) lines. A similar situation occurs in the diagrammatic technique with spin operators.[13]

This information about the rules operating in the diagrammatic technique is sufficient for what follows.

3. VERTEX PARTS IN THE GRPA

In Ref. 3 we suggested for the t–J model the generalized random phase approximation (GRPA) and used it to calculate the spin Green's function from (2.4), the dy-

namic susceptibility. Here we use it to calculate the electron Green's function (2.4). The essence of the GRPA is the summation of all the diagrams containing electron loops (similar to RPA in the theory of a Fermi liquid). For the t–J model summation of loop diagrams is not a trivial problem, since there are four types of electron loops. This becomes quite obvious if we set up the Bethe–Salpeter equation for the particle–hole channel,

$$\tag{3.1}$$

with the initial four-leg diagram

$$\tag{3.2}$$

Iterating (3.1), we see that exactly four loops emerge:

$$\tag{3.3}$$

In the series generated by Eq. (3.1) all diagrams are chains in which the loops (3.3) are connected by wavy or dotted lines, with the result that the effective four-leg diagram is expressed in terms of the quantities (3.3) depending on one transfer momentum k. We therefore arrive at the following expression:[3]

$$\equiv \Gamma(k_{1} - k\ k_{1}; k_{2} + k, k_{2})$$

$$= \frac{1}{d^{0}(k)} \{ \varepsilon(\mathbf{k}_{1} - \mathbf{k}) \varepsilon(\mathbf{k}_{2} + \mathbf{k}) \Pi(k)$$

$$+ \varepsilon(\mathbf{k}_{1} - \mathbf{k})[1 - Q(k)]$$

$$+ \varepsilon(\mathbf{k}_{2} + \mathbf{k})[1 - \Lambda(k)]$$

$$+ \Phi(k) + J(\mathbf{k}) \}, \tag{3.4}$$

where

$$d^{0}(k) = [1 - \Lambda(k)][1 - Q(k)] - \Pi(k)[\Phi(k) + J(\mathbf{k})], \tag{3.5}$$

and the quantities Π, Q, Λ, Φ are expressed in terms of the electron Green's functions as follows:

$$\begin{pmatrix} \Pi(k) \\ Q(k) \\ \Lambda(k) \\ \Phi(k) \end{pmatrix} = \frac{T}{N} \sum_{k_1} \begin{pmatrix} 1 \\ \varepsilon(\mathbf{k}_1) \\ \varepsilon(\mathbf{k}_1 - \mathbf{k}) \\ \varepsilon(\mathbf{k}_1)\varepsilon(\mathbf{k}_1 - \mathbf{k}) \end{pmatrix} G_\uparrow(k_1 - k) G_\downarrow(k_1).$$

$$(3.6)$$

In a similar approximation we must sum the series for effective three-leg diagrams. These are expressed in terms of the four-leg diagram found above via the following diagram relations:

$$(3.7)$$

$$(3.8)$$

with the initial three-leg diagrams

$$(3.9)$$

$$(3.10)$$

Substituting the result (3.4) into Eqs. (3.7) and (3.8), we get

 $\equiv \gamma_2(k_1 - k\, k_1; k)$

$$= \frac{1}{d^0(k)} \{\varepsilon(\mathbf{k}_1 - \mathbf{k})[1 - Q(k)]$$

$$+ \Phi(k) + J(\mathbf{k})\}, \qquad (3.11)$$

 $\equiv \gamma_1(k; k_2 + k\, k_2)$

$$= \frac{\langle B^{+-}\rangle_0}{d^0(k)} \{\varepsilon(\mathbf{k}_2 + \mathbf{k})[1 - \Lambda(k)]$$

$$+ \Phi(k) + J(\mathbf{k})\}. \qquad (3.12)$$

In addition to the four-leg diagram (3.1) describing the effective electron interaction in the singlet channel we must calculate the four-leg diagram for the triplet channel, which is needed to describe charge fluctuations and fluctuations of the longitudinal spin components. In the GRPA this four-leg diagram is determined by the following system of equations:

$$(3.13)$$

$$(3.14)$$

with the initial vertex part

$$(3.15)$$

It is clear that now all the elementary vertex parts from Fig. 1 are included. The last thing to take into account is the renormalization of the simplest three-point vertices. Within the GRPA,

$$(3.16)$$

with the initial vertex part

$$(3.17)$$

In exactly the same manner we must renormalize the vertex for the other orientation of spin.

The vertex part determined by Eqs. (3.13)–(3.17) were calculated in Ref. 4 in connection with the problem of superconductivity in the t–J model. Here are the results for the three-leg diagram:

 $\equiv \gamma_\parallel^{\sigma+}(k; k_2 + k\, k_2)$

$$= \frac{\langle F^{\sigma 0}\rangle_0}{d^0(k) d_c^0(k)} \{\varepsilon(\mathbf{k}_2 + \mathbf{k})(1 - \Lambda^2 - \Pi\Phi$$

$$- J\Lambda\Pi) + \Phi(\Lambda + Q) + J(1 + \Lambda Q)\}, \qquad (3.18)$$

where $d^0(k)$ is defined by (3.5), and

$$d_c^0(k) = [1 + \Lambda(k)][1 + Q(k)] - \Pi(k)[\Phi(k) - J(\mathbf{k})]. \qquad (3.19)$$

The quantities Π, Λ, Q, and Φ are loops of the form (3.3), but with the same spin at the electron lines. Since we consider the paramagnetic phase in the absence of an external field, the set of quantities entering into (3.18) and (3.19) coincides with that entering into Eqs. (3.4)–(3.6). Note that in all the analytical expressions representing the vertex parts (3.13)–(3.15) the denominator contains the factor $d_c^0(k)$ together with $d^0(k)$. As shown in Ref. 5, the factor $d^0(k)$ is related to the denominator of the magnetic susceptibility and the factor $d_c^0(k)$ to the denominator of the dielectric susceptibility.
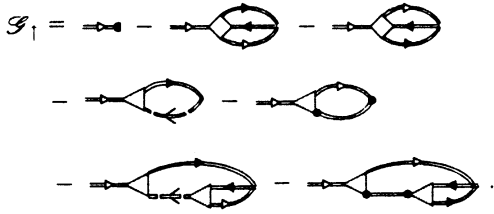
FIG. 2. Diagrammatic representation of the electron Green's function.

4. THE ELECTRON GREEN'S FUNCTION

In analyzing the diagrammatic structure of the Green's functions defined by Eqs. (2.4) and (2.5) it must be kept in mind that when the commutators of the operators are not c-numbers, diagrams with terminal parts irrevocably emerge since there are several types of external vertices. For instance, for the electron Green's function $\mathscr{G}_\uparrow$ the sum of the diagrams in the GRPA transforms into a compact form (Fig. 2). Each heavy fermion and boson line here satisfies the Dyson equation with the self-energy parts $\Sigma_\uparrow$ and $\Sigma_\downarrow$ (Fig. 3). Finally, the double line connecting two heavy dots (corresponding to operators $F^{\sigma 0}$ and $F^{\sigma' 0}$) is the second-order total cumulant, which obeys an equation of the Dyson type with a matrix self-energy part $\Sigma_{\sigma\sigma'}$. (To exclude the possibility of allowing for terms in the diagrammatic expressions for $\mathscr{G}_\uparrow$ and $\Sigma_\uparrow$ twice, some first- and second-order diagrams, not given here, must be subtracted).

As Figs. 2 and 3 show, the terminal part of the Green's function $\mathscr{G}_\uparrow$ and all self-energy parts are expressed in terms of a common system of vertex parts calculated in Sec. 3 within the GRPA. The exotic form of the diagrammatic expression for $\mathscr{G}_\uparrow$ should not be surprising since it corresponds to the Green's function of physical electrons defined on X-operatorsrather than on Fermi operators. Terminal parts appear in the Green's functions for other models, too, if they are defined on X-operators (say, in the Anderson model), where the slave-boson representation is employed.[15] Note that the expression for $\mathscr{G}_\uparrow$ was obtained from the general diagrammatic representation for the electron Green's function[6] in the GRPA for four-leg diagrams. We also note that in the diagrams in Figs. 2 and 3 all electron scattering processes are taken into account: electron–electron scattering, scattering on transverse and longitudinal spin fluctuations, and scattering on charge fluctuations.
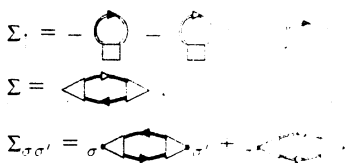

FIG. 3. Self-energy parts for the electron propagator ($\Sigma_\uparrow$) and the propagators of transverse (Σ) and longitudinal ($\Sigma_{\sigma\sigma'}$) spin deviations.

If into the diagrams in Figs. 2 and 3 we substitute all the vertex parts calculated in Sec. 3, after fairly involved calculations we arrive at the following simple result:

$$\mathscr{G}_\uparrow(k) = \frac{\langle F^{+0}\rangle + \Delta_\uparrow(k)}{[G^0_\uparrow(k)]^{-1} - \Sigma_\uparrow(k)}, \tag{4.1}$$

where the expressions

$$\Delta_\uparrow(k) = \frac{T}{N}\sum_{k_1}\left(\frac{A(k,k_1)}{d(k_1)} + \frac{A_c(k,k_1)}{d_c(k_1)} + S_\Delta(k,k_1)\right)$$
$$\times G_\downarrow(k+k_1), \tag{4.2}$$

$$\Sigma_\uparrow(k) = \frac{T}{N}\sum_{k_1}\left(\frac{V(k,k_1)}{d(k_1)} + \frac{V_c(k,k_1)}{d_c(k_1)} + S_\Sigma(k,k_1)\right)G_\downarrow(k+k_1) \tag{4.3}$$

are the terminal and self-energy parts of the Green's function.

The quantities $d(k)$ and $d_c(k)$ are also the denominators of the magnetic and dielectric susceptibilities, calculated in Refs. 3 and 5:

$$\chi(k) = \frac{\chi^0(k)}{d(k)}, \chi_c(k) = \frac{\chi^0_c(k)}{d_c(k)}, \tag{4.4}$$

with

$$d(k) = (1-\Lambda(k))(1-Q(k)) + \chi^0(k)[\Phi(k)+J(\mathbf{k})], \tag{4.5}$$

$$d_c(k) = [1+\Lambda(k)](1+Q(k)) + \chi^0_c(k)[\Phi(k)-J(\mathbf{k})], \tag{4.6}$$

and $\chi^0(k)$ and $\chi^0_c(k)$ the initial susceptibilities,

$$\chi^0(k) = \frac{n_0}{2T}\delta_{\omega_n,0} - \Pi(k), \tag{4.7}$$

$$\chi^0_c(k) = \frac{n_0(1-n_0)}{2T}\delta_{\omega_n,0} - \Pi(k). \tag{4.8}$$

In the last two formulas the factor n_0 is a function of the parameter μ/T:

$$n_0 = \frac{2\exp(\mu/T)}{1+2\exp(\mu/T)}. \tag{4.9}$$

The amplitudes in Eqs. (4.2) and (4.3) are expressed in terms of Π, Q, Λ, and Φ as follows:

$$A(k,k_1) = \tfrac{1}{2}\{\chi^0(k_1)[\varepsilon(\mathbf{k}_1+\mathbf{k}) + \Phi(k_1)+J(\mathbf{k}_1)]$$
$$-\Lambda(k_1)[1-Q(k_1)]\},$$

$$A_c(k,k_1) = \tfrac{1}{2}\{\chi^0_c(k_1)[\varepsilon(\mathbf{k}_1+\mathbf{k}) - \Phi(k_1)+J(\mathbf{k}_1)]$$
$$-\Lambda(k_1)[1+Q(k_1)]\},$$

$$V(k,k_1) = \tfrac{1}{2}\{\chi^0(k_1)\varepsilon(\mathbf{k})\varepsilon(\mathbf{k}_1+\mathbf{k}) - \varepsilon(\mathbf{k})[1-Q(k_1)]$$
$$-\varepsilon(\mathbf{k}_1+\mathbf{k})[1-\Lambda(k_1)] - \Phi(k_1)-J(\mathbf{k}_1)\},$$

$$V_c(k,k_1) = \tfrac{1}{2}\{\chi^0_c(k_1)\varepsilon(\mathbf{k})\varepsilon(\mathbf{k}_1+\mathbf{k}) + \varepsilon(\mathbf{k})[1+Q(k_1)]$$
$$+\varepsilon(\mathbf{k}_1+\mathbf{k})[1+\Lambda(k_1)] - \Phi(k_1)+J(\mathbf{k}_1)\}.$$

Two more expressions represent the first- and second-order diagrams and ensure that the contributions in the diagrammatic expressions for $\mathscr{G}_\uparrow$ and $\Sigma_\uparrow$ are not counted twice:

$$S_\Delta(k,k_1)=\varepsilon(\mathbf{k}+\mathbf{k}_1)\Pi(k_1)+\Lambda(k_1),$$

$$S_\Sigma(k,k_1)=\varepsilon(\mathbf{k})\varepsilon(\mathbf{k}+\mathbf{k}_1)\Pi(k_1)+\varepsilon(\mathbf{k})\Lambda(k_1)$$

$$+\varepsilon(\mathbf{k}+\mathbf{k}_1)Q(k_1)+\Phi(k_1)-J(0).$$

Let us now discuss the result (4.1) for the electron Green's function. In it the cumulant $\langle F^{+0}\rangle=1-n_\downarrow$ is equal to $1-n/2$ for the paramagnetic phase. If we ignore $\Sigma_\uparrow$ and $\Delta_\uparrow$, expression (4.1) represents the Green's function in the Hubbard-I approximation with the spectrum

$$\xi(\mathbf{k})=(1-\tfrac{1}{2}n)\varepsilon(\mathbf{k}).\qquad(4.10)$$

The complete expression (4.1) allows for the corrections in the GRPA. Formally these corrections have the same structure as in the RPA for a Fermi liquid. In both cases they are expressed in terms of the dynamics magnetic and dielectric susceptibilities.[16-18] Note that the corrections in the numerator and denominator of $\Delta_\uparrow$ and $\Sigma_\uparrow$ are of the same order of magnitude, which suggests the impossibility of ignoring the terminal contributions. While the self-energy part $\Sigma_\uparrow$ determines a pole in the Green's function, the terminal part $\Delta_\uparrow$ gives the residue at this pole and is extremely important in counting the number of states. We will have the opportunity to see this directly in what follows. In the limit $U\to\infty$, if we ignore longitudinal spin fluctuations and charge fluctuations, Eqs.(4.1)–(4.3) transform into those derived earlier in Ref. 6.

Note that the electron and spin Green's functions are expressed in the GRPA in terms of the four quantities $\Pi(k)$, $Q(k)$, $\Lambda(k)$, and $\Phi(k)$ defined in (3.6). The fermion Green's function G(k) entering into these quantities obeys the Dyson equation and is given by

$$G(k)=\frac{1}{i\omega_n-\xi(\mathbf{k})-\Sigma(k)+\mu},\qquad(4.11)$$

where $\Sigma(k)$ is given by formula (4.3) in which the spin index should be dropped. The quantity $G(k)$ and the four loops Π, Q, Λ, and Φ depending on it must be determined self-consistently.

5. MAGNETIC PHASE TRANSITIONS IN THE t–J MODEL

The GRPA corrections to the self-energy are expressed in terms of the magnetic and dielectric susceptibilities and, therefore, become essential near magnetic or dielectric phase transitions. Since we wish to study electronic states near a magnetic phase transition, we begin by studying magnetic phase transitions in the t–J model (more exactly, we calculate the Curie temperature T_C and the Néel temperature T_N as functions of the model parameters and establish the nature of the phase transitions) and then return to studying the electronic states of the system near ferromagnetic and antiferromagnetic phase transitions.

The simplest way to describe a system with spontaneously broken symmetry is to employ the mean-field approximation. Let us set up a self-consistent equation for the
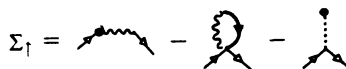

$$\Sigma_\uparrow = $$

FIG. 4. The self-energy part of the fermion Green's function in the mean-field approximation.

fermion Green's function G_σ that obeys the Dyson equation with a self-energy part Σ_σ shown in Fig. 4. A similar diagrammatic expression can be written for $\Sigma_\downarrow$ by changing the "color" of the arrows in the expression for $\Sigma_\uparrow$. Each diagram in Fig. 4 is independent of four-momentum. The heavy line in the second diagram in Fig. 4 corresponds to a refined Green's function $G_\downarrow$. The heavy dots in the first and third diagrams in Fig. 4 correspond to the cumulants $\langle F^{+0}\rangle$ and $\langle F^{-0}\rangle$, for which we must also write self-consistent equations by adding diagrammatic series for $\langle X^{++}\rangle$ and $\langle X^-\rangle$ with the same diagram elements that define $\Sigma_\uparrow$ and $\Sigma_\downarrow$ (Fig. 5). Here each external vertex corresponds to operator X^{++}. Note that the series for $\langle X^{++}\rangle$ contains "heavier" Green lines; hence, the equations for $G_\uparrow$ and $G_\downarrow$ and the series for $\langle X^{++}\rangle$ and $\langle X^{--}\rangle$ constitute a system of coupled self-consistent equations. An analysis of the series of Fig. 5 shows that it is a Taylor series for the function represented by a zero-approximation diagram.

We begin with the ferromagnetic phase. We write the Green's function in the form

$$G_\sigma(k)=\frac{1}{i\omega_n-\xi_\sigma(\mathbf{k})-\Delta_\sigma+\mu},\qquad(5.1)$$

where Δ_σ satisfies the equation

$$\Delta_\sigma=-zJn_{-\sigma}-\frac{1}{N}\sum_\mathbf{k}\varepsilon(\mathbf{k})f[\xi_{-\sigma}(\mathbf{k})+\Delta_{-\sigma}].\qquad(5.2)$$

Here $f(\xi)$ is the Fermi function. We have allowed for the fact that $\langle X_i^{\sigma\sigma}\rangle=n_\sigma$ is the mean number of electrons with spin σ at a site, and

$$\xi_\sigma(\mathbf{k})=(1-n_{-\sigma})\varepsilon(\mathbf{k})$$

the energy of an electron in the ferromagnetic phase in the Hubbard-I approximation.

We set up the equations for the order parameters

$$\Delta=\Delta_\uparrow-\Delta_\downarrow,\ m=n_\uparrow-n_\downarrow:\qquad(5.3)$$
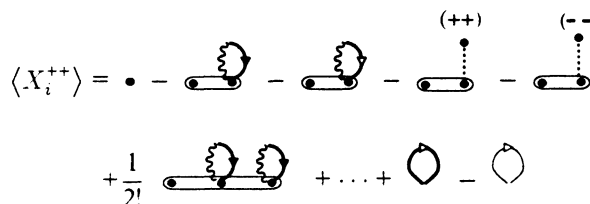

$$\langle X_i^{++}\rangle = $$

FIG. 5. The sum of diagrams for the cumulant in the mean-field approximation.

namely,

$$\Delta = -zJm + \frac{1}{N}\sum_{\mathbf{k}}\varepsilon(\mathbf{k})\left\{f\left[\xi(\mathbf{k}) + \frac{\Delta - m\varepsilon(\mathbf{k})}{2}\right]\right.$$

$$\left. -f\left[\xi(\mathbf{k}) - \frac{\Delta - m\varepsilon(\mathbf{k})}{2}\right]\right\}, \qquad (5.4)$$

$$m = n_0\left(x,\frac{\Delta}{2T}\right)\tanh\frac{\Delta}{2T} + \left[f\left(\frac{\Delta}{2} - f\left(-\frac{\Delta}{2}\right)\right)\right]$$

$$-\frac{1}{N}\sum_{\mathbf{k}}\left\{f\left[\xi(k)\right.\right.$$

$$\left.+\frac{\Delta - m\varepsilon(\mathbf{k})}{2}\right] - f\left[\xi(\mathbf{k}) - \frac{\Delta - m\varepsilon(\mathbf{k})}{2}\right]\right\}, \qquad (5.5)$$

where

$$n_0(x,\eta) = \frac{2\cosh\eta\exp(\mu/T)}{1 + 2\cosh\eta\exp(\mu/T)} \qquad (5.6)$$

transforms into formula (4.9) for n_0 at $\Delta = 0$, that is, in the paramagnetic phase.

We linearize Eqs. (5.4) and (5.5) in Δ and m. Then they can be written as

$$[1 - \Lambda(0,0)]m = \left[\frac{n_0}{2T} - \Pi(0,0)\right]\Delta, \qquad (5.7)$$

$$[1 - \Lambda(0,0)]\Delta = -[\Phi(0,0) + zJ]m,$$

where we have introduced the notation

$$\{\Pi(0,0),\Lambda(0,0),\Phi(0,0)\}$$

$$= \frac{1}{N}\sum_{\mathbf{k}}\{1,\varepsilon(\mathbf{k}),\varepsilon^2(\mathbf{k})\}f'[\xi(\mathbf{k})] \qquad (5.8)$$

(f'(ξ) is the derivative of the Fermi function with respect to the argument). Note that the quantities specified in (5.8) are particular values of the quantities (3.6) at zero momentum and frequency. Equations (5.7) lead to the following equation:

$$[1 - \Lambda(0,0)]^2 + \left[\frac{n_0}{2T} - \Pi(0,0)\right](\Phi(0,0) + zJ) = 0, \qquad (5.9)$$

which specifies the line of the phase transition into the paramagnetic phase. It coincides with the equation determining the condition for the divergence of the DC magnetic susceptibility (4.4) of the paramagnetic phase at $\mathbf{k} = 0$. The fact that these equations coincide indicates a second-order phase transition. Equation (5.9) leads to an expression for the Curie temperature:

$$T_C = -\frac{n_0}{2}\frac{\Phi(0,0) + zJ}{[1 - \Lambda(0,0)]^2 - \Pi(0,0)(\Phi(0,0) + zJ)}. \qquad (5.10)$$

From (5.8) it is clear that the denominator in (5.10) is positive and $\Phi(0,0) < 0$. Thus, Eq. (5.10) shows that ferromagnetic ordering is of a kinetic nature and that the effective exchange interaction inhibits it.

Now let us study the antiferromagnetic phase with the wave vector $\mathbf{Q} = (\pi,\pi,\pi)/a$. The order parameter m is defined by the condition

$$\langle X_i^{++}\rangle - - \langle X_i^-\rangle = mp_i, \qquad (5.11)$$

where pi $= \exp(-i\mathbf{Q}\cdot\mathbf{R}_i)$ assumes two values, $+1$ and -1. This leads to a situation in which the Green's function $G_\sigma(k)$ determined by mean-field equations (Figs 4 and 5) is a 2-by-2 matrix:

$$\hat{G}_\sigma(k) = \frac{1}{d_A(k)}$$

$$\times\begin{pmatrix} i\omega_k + \mu + \xi(\mathbf{k}) & \sigma[-\Delta - \tfrac{1}{2}m\varepsilon(\mathbf{k})] \\ \sigma[-\Delta + \tfrac{1}{2}m\varepsilon(\mathbf{k})] & i\omega_k + \mu - \xi(\mathbf{k}) \end{pmatrix}, \qquad (5.12)$$

where

$$d_A(k) = (i\omega_k + \mu)^2 - E^2(\mathbf{k}), \qquad (5.13)$$

$$E(\mathbf{k}) = \sqrt{[(1 - \tfrac{1}{2}n)^2 - \tfrac{1}{2}m^2]\varepsilon^2(\mathbf{k}) + \Delta^2}.$$

The order parameters m (the magnetization of the sublattice) and Δ (the gap in the electron spectrum) can be found from the following equations:

$$\Delta = \frac{m}{4N}\sum_{\mathbf{k}}\varepsilon^2(\mathbf{k})\frac{f[E(\mathbf{k})] - f[-E(\mathbf{k})]}{E(\mathbf{k})} + \tfrac{1}{2}zJm, \qquad (5.14)$$

$$m = -\Delta\frac{1}{N}\sum_{\mathbf{k}}\frac{f[E(\mathbf{k})] - f[-E(\mathbf{k})]}{E(\mathbf{k})}$$

$$+ n_0\left(\frac{\mu}{T},\frac{\Delta}{T}\right)\tanh\frac{\Delta}{T} + [f(\Delta) - f(-\Delta)]. \qquad (5.15)$$

Linearization of these equations leads to the equation for the boundary of the antiferromagnetic phase,

$$1 - \left[\frac{n_0}{2T} - \Pi(\mathbf{Q},0)\right][\Phi(\mathbf{Q},0) - zJ] = 0, \qquad (5.16)$$

which also coincides with the condition for the divergence of the DC magnetic susceptibility of the paramagnetic phase at $\mathbf{k} = \mathbf{Q}$. From this we can find the Néel temperature:

$$T_N = \frac{n_0}{2}\frac{zJ - \Phi(\mathbf{Q},0)}{1 - \Pi(\mathbf{Q},0[\Phi(\mathbf{Q},0) - zJ]}, \qquad (5.17)$$

where

$$\Pi(\mathbf{Q},0) = \frac{1}{1 - n/2}\int d\varepsilon\, \rho_0(\varepsilon)\frac{1}{\varepsilon}f[\xi(\varepsilon)], \qquad (5.18)$$

$$\Phi(\mathbf{Q},0) = -\frac{1}{1 - n/2}\int d\varepsilon\, \rho_0(\varepsilon)\varepsilon f[\xi(\varepsilon)].$$

In view of the fact that $\Pi(\mathbf{Q},0) < 0$ and $\Phi(\mathbf{Q},0) > 0$, the denominator in (5.17) is positive, and from (5.17) it follows that the nature of antiferromagnetic ordering in the

t–J model is entirely different from that of ferromagnetic ordering. The reason lies in the indirect ferromagnetic exchange, while the motion of electrons only inhibits such exchange.

Equation (5.17) determines the dependence of T_N on n. For a half-filled band ($n=1$),

$$T_N^0 = \frac{1}{2} \frac{zJ}{1+\ln 2} \qquad (5.19)$$

(the factor $\ln 2$ appears because in the quantity $\Phi(Q,0)$ in Eq. (5.17) we allowed for the term linear in T). When there are few holes ($1-n \ll 1$)

$$T_N = \frac{1}{2} \frac{2zJ-(1-n)zt}{1+\ln 2} . \qquad (5.20)$$

Because of the large coefficient of $1-n$, the decrease in T_N with an increasing hole concentration occurs very rapidly. At the electron concentration

$$n_A = 1-\kappa \quad (\kappa \equiv t/U \ll 1)$$

the Néel temperature T_N vanishes. Near n_A this temperature is a linear function of n:

$$T_N = \tfrac{1}{2}(n-n_A)zt. \qquad (5.21)$$

Thus, near $n=1$ there is antiferromagnetic ordering in the interval $n_A < n < 1$. The ferromagnetic state exists in the interval $n_c < n < n_F$, where n_F is defined by the equation

$$2ztp_0(n_Fzt) = \kappa. \qquad (5.22)$$

These intervals can overlap, but near $n=1$ a purely antiferromagnetic state is realized. In the overlap region, T_N may be much higher than T_C for fairly large κ. It can also be demonstrated that for low temperatures $T \ll T_N^0$ and for $n_A \approx 1$, the correlation length of antiferromagnetic fluctuations,

$$l_{cA} \sim \frac{a}{\sqrt{1-n}}, \qquad (5.23)$$

is determined by the hole concentration and depends weakly on temperature.

Let us now examine the magnetic phase transitions occurring because of temperature variations. According to (4.4), the DC magnetic susceptibility of the paramagnetic phase in the vicinity of the wave vectors $\mathbf{k}=0$ and $\mathbf{k}=\mathbf{Q}$ can be represented in the form

$$\chi(\mathbf{k},0) = \frac{n_0}{\alpha + \beta(\mathbf{k}a)^2}, \qquad (5.24)$$

$$\chi_A(\mathbf{k},0) = \frac{n_0}{\alpha_A + \beta_A a^2(\mathbf{k}-\mathbf{Q})^2}, $$

with β and β_A positive, and α and α_A change sign at the phase-transition point:

$$\alpha = 2[1-\Lambda(0,0)]^2(T-T_C), \quad \alpha_A = 2(T-T_N). \qquad (5.25)$$

The magnetic correlation length near a ferromagnetic or antiferromagnetic phase transition is determined by the following formulas:

$$l_C = \sqrt{\alpha/\beta a}, \quad l_{CA} = \sqrt{\alpha_A/\beta_A a}, \qquad (5.26)$$

with β and β_A of the order of T_C and T_N, respectively (the explicit expressions are not given here).

6. THE ELECTRON SYSTEM NEAR A MAGNETIC PHASE TRANSITION

Let us now return to Eqs. (4.1)–(4.3) for the electron Green's function in the paramagnetic phase and consider them near a magnetic phase transition. In Eq. (4.3) in this case the quasistatic contribution from magnetic fluctuations dominates. Retaining only this contribution, we can write Eq. (4.3) as

$$\Sigma(\mathbf{k},\omega) = \frac{3}{2} \frac{T}{N} \sum_{\mathbf{k}_1} \varepsilon(\mathbf{k})\varepsilon(\mathbf{k}+\mathbf{k}_1)\chi(\mathbf{k}_1;0)G(\mathbf{k}+\mathbf{k}_1;\omega). \qquad (6.1)$$

(From now on we deal with the retarded Green's function. The transformation is done via an analytic continuation $i\omega_n \to \omega + i\delta$ onto the real axis). A similar expression in the Hubbard model for $U \ll t$ was derived in Ref. 16, and for $U \gg t$ in Refs. 17 and 18, where it was used to study the metal–insulator phase transition in the $U \sim t$ region.

In the same approximations, from Eq. (4.2) we find a simple relationship between Δ and Σ:

$$\Delta(\mathbf{k};\omega) = \sum (\mathbf{k};\omega)/\varepsilon(\mathbf{k}) . \qquad (6.2)$$

In the integral equation (6.1) it is sufficient to concentrate only on integration over a small neighborhood of the $\mathbf{k}_1$-space near the point $\mathbf{k}_1 = 0$ in the case of ferromagnetic instability and the point $\mathbf{k}_1 = \mathbf{Q}$ in the case of antiferromagnetic instability ($\mathbf{Q}$ is the wave vector of the antiferromagnetic structure). We start with ferromagnetic instability. Taking the slowly varying function $G(\mathbf{k})$ outside the sum in (6.1), we go from Eq. (6.1) to the following:

$$\Sigma(\mathbf{k};\omega) = \frac{b\varepsilon^2(\mathbf{k})}{\omega - \xi(\mathbf{k}) - \Sigma(\mathbf{k};\omega)}, \qquad (6.3)$$

where we have introduced the notation

$$b = \frac{3}{3} \frac{T}{N} \sum_{\mathbf{k}_1} \chi(\mathbf{k}_1;0). \qquad (6.4)$$

(Summation in (6.4) is done over the neighborhood of the vector $\mathbf{k}_1 = 0$.) When writing (6.3), we change the energy reference point:

$$\omega + \mu \to \omega.$$

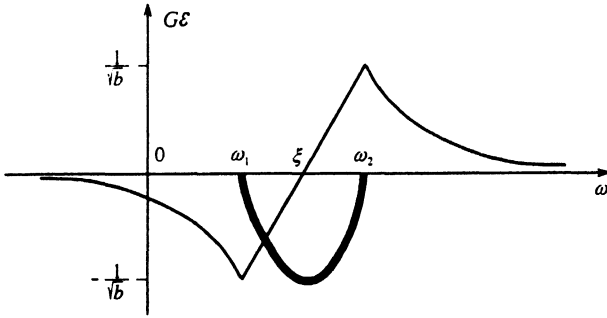The solution to Eq. (6.3) yields an explicit expression for the Green's function:

FIG. 6. The real part (light curve) and the imaginary part (heavy curve) of the Green's function near a ferromagnetic phase transition.

$$G(k)=\frac{1}{2b\varepsilon^2(k)}$$

$$\times \begin{cases} \omega-\xi(k)-i\sqrt{-X(k)}, & \omega_1(k)<\omega<\omega_2(k), \\ \omega-\xi(k)-\text{sign}\,[\omega-\xi(k)]\sqrt{X(k)}, & \\ \omega<\omega_1(k), & \omega>\omega_2(k), \end{cases}$$

$$\tag{6.5}$$

where

$$X(k)=[\omega-\omega_1(k)][\omega-\omega_2(k)],$$

$$\tag{6.6}$$

$$\omega_{1,2}(k)=\xi(k)\mp 2\sqrt{b}\,\varepsilon(k).$$

The frequency dependence of G is depicted in Fig. 6. We see that owing to ferromagnetic fluctuations the Green's function is of a nonquasiparticle (incoherent) nature. The quantity b, the measure of fluctuations, also determines the extent to which G is incoherent. Since $\omega_1 \to \omega_2$ as $b\to 0$, the imaginary part of G is a narrow delta-like peak, and we have returned to the quasiparticle nature of electronic states, described by the Hubbard-I approximation.

Near antiferromagnetic instability we must set up equations for two quantities,

$$\Sigma=\Sigma(k;\omega), \quad \Sigma'=\Sigma(k+Q;\omega).$$

The general expression (6.1) then yields the equations for Σ and Σ':

$$\Sigma=\frac{-b\varepsilon^2}{\omega+\xi-\Sigma'}, \quad \Sigma'=\frac{-b\varepsilon^2}{\omega-\xi-\Sigma}. \tag{6.7}$$

Excluding Σ', we arrive at a quadratic equation for Σ similar to the equation for the case of ferromagnetic instability, where in the latter we must do the substitution

$$b \to -\frac{\omega-\xi}{\omega+\xi}\,b. \tag{6.8}$$

Thus, for G we arrive at a result similar to (6.5):

$$G=-\frac{1}{2b\varepsilon^2}\frac{\omega+\xi}{\omega-\xi}$$

$$\times \begin{cases} \omega-\xi-i\sqrt{-Y}, & \omega_0<|\omega|<\xi, \\ \omega-\xi-\text{sign}\,(\omega-\xi)\sqrt{Y}, & |\omega|<\omega_0,\ |\omega|>\xi, \end{cases}$$

$$\tag{6.9}$$

where

$$Y=\frac{\omega-\xi}{\omega+\xi}(\omega^2-\omega_0^2), \quad \omega_0=\sqrt{(1-\tfrac{1}{2}n)^2-4b\varepsilon}. \tag{6.10}$$

The fluctuation measure b is determined by the same expression (6.4) but with summation now over the neighborhood of vector $k=Q$. In the expression for the Green's function there are two frequency regions in the neighborhood of $\omega=\pm\xi$ where the imaginary part of G is finite. The width of each is of the order of b. As $b\to 0$, the peak in the density of states near $\omega=\xi$ degenerates into a delta function and the peak at $\omega=-\xi$ disappears, so that we again arrive at the quasiparticle structure of the Hubbard-I approximation. The presence of two ranges in Im G is an indication of the two-pole expression for the Green's function of the future antiferromagnetic phase. If we introduce the quantity

$$m=4\sqrt{b}, \tag{6.11}$$

formula (6.10) for $\omega_0(k)$ coincides with the expression for the spectrum of electrons in the antiferromagnetic phase, where only one order parameter, the sublattice's magnetization m, is taken into account. In exactly the same way formula (6.6) coincides with the expression for the spectrum of electrons in the ferromagnetic phase for two orientations of spin. Thus, there is a certain correspondence between the electron spectra of the ferromagnetic and antiferromagnetic phases and the characteristic frequencies (determining the boundaries for incoherent states) of the electron spectrum in the paramagnetic phase near magnetic phase transitions. According to the definition (6.11), m must be interpreted as the value of magnetization (of the sublattice) in a region of the order of the correlation length.

Let us now calculate the parameter b. According to the definition (6.4) and the first formula in (5.24), for the case of ferromagnetic instability we have

$$b=n_0\frac{3Tk_0a^3}{4\pi^2\beta}\left(1-\frac{1}{k_0l_C}\text{arctg}k_0l_C\right), \tag{6.12}$$

where k_0 is the cutoff parameter.

In formulas (5.10) and (5.17) the quantities Φ, Λ, and Π depend on the temperature directly and through the parameter b. Hence, these formulas must be considered equations for finding T_C and T_N. Let us now calculate Φ, Λ, and Π, which are expressed in terms of the Green's function G_σ via Eqs. (3.6). In the case of ferromagnetic instability, to calculate $\Pi(0,0)$, $\Lambda(0,0)$, and $\Phi(0,0)$ we must sum over discrete frequencies in $T\Sigma_n G^2(q;i\omega_n)$, where the Green's function is given by (6.5). To this end we consider the following integral in the complex z plane:
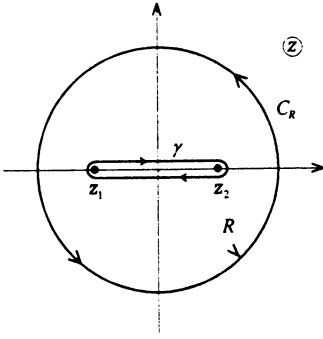
FIG. 7. The integration contour in Eq. (5.20).

$$\int_\Gamma \frac{dz}{2\pi i} G^2[\mathbf{q};z+\xi(\mathbf{q})]f[z+\xi(\mathbf{q})], \qquad (6.13)$$

where

$$G^2[\mathbf{q};z+\xi(\mathbf{q})] = \frac{z^2-2b\varepsilon^2(\mathbf{q})-z\sqrt{z^2-4b\varepsilon^2(\mathbf{q})}}{2b^2\varepsilon^4(\mathbf{q})},$$

and the contour Γ consists of a circle C_R with a large radius R and the contour bypassing two branch points,

$$z_{1,2}(\mathbf{q}) = \mp 2\sqrt{b}\,\varepsilon(\mathbf{q}), \qquad (6.14)$$

as shown in Fig. 7.

Using the residue theorem and taking into account the dual-sign nature of the square-root function, we reduce the summation over discrete frequencies to integration along a real-number interval:

$$T\sum_n G^2(\mathbf{q};i\omega_n)$$

$$=\frac{1}{2\pi b^2\varepsilon^4(\mathbf{q})}\int_{z_1(\mathbf{q})}^{z_2(\mathbf{q})} dz\, z\sqrt{(z_2(\mathbf{q})-z)[z-z_1(\mathbf{q})]}$$

$$\times f[z+\xi(\mathbf{q})]. \qquad (6.15)$$

For $b \ll 1$ the expression can be expanded in a series:

$$T\sum_n G^2(\mathbf{q};i\omega_n) = f'[\xi(\mathbf{q})]+\tfrac{1}{3}\varepsilon^2(\mathbf{q})f'''[\xi(\mathbf{q})]b+\cdots,$$

$$(6.16)$$

where the primes denote the derivatives of $f(z)$. Substituting (6.16) into (3.6), we arrive at the following expressions for the loops:

$$\Pi(0,0)=\Pi_0+\Pi_1 b+\cdots,$$

$$\Lambda(0,0)=\Lambda_0+\Lambda_1 b+\cdots, \qquad (6.17)$$

$$\Phi(0,0)=\Phi_0+\Phi_1 b+\cdots,$$

where

$$\{\Pi_0,\Lambda_0,\Phi_0\}=\frac{1}{N}\sum_{\mathbf{q}}\{1,\varepsilon(\mathbf{q}),\varepsilon^2(\mathbf{q})\}f'[\xi(\mathbf{q})], \qquad (6.18)$$

$$\{\Pi_1,\Lambda_1,\Phi_1\}=\frac{1}{3}\frac{1}{N}\sum_{\mathbf{q}}\{\varepsilon^2(\mathbf{q}),\varepsilon^3(\mathbf{q}),\varepsilon^4(\mathbf{q})\}f'''[\xi(\mathbf{q})].$$

$$(6.19)$$

If we ignore the temperature dependence of the coefficients of b in (6.17), the quantities Π_1, Λ_1, and Φ_1 can be expressed in terms of the density of states $\rho_0(\varepsilon)$ in the initial spectrum $\varepsilon(\mathbf{q})$:

$$\{\Pi_1,\Lambda_1,\Phi_1\}=\{\tfrac{2}{3},2\widetilde{\mu},\ 4\widetilde{\mu}^2\}\,\rho_0(\widetilde{\mu})/(1-\tfrac{1}{2}n)^3, \qquad (6.20)$$

where $\widetilde{\mu}=\mu(l(1-\tfrac{1}{2}n)$. Now substituting (6.17) into (5.10), we find the correction to the Curie temperature caused by the quasistatic spin fluctuations:

$$T_C=T_C^0-\frac{2n_0\widetilde{\mu}\rho_0(\widetilde{\mu})(\widetilde{\mu}+zJ)}{[\widetilde{\mu}\rho_0(\widetilde{\mu})+(1-\tfrac{1}{2}n)^3}b. \qquad (6.21)$$

Here T_C^0 is the Curie temperature defined by Eq. (5.10) without allowing for these fluctuations (i.e., for $b\to 0$). We see that the fluctuations narrow the range for a magnetically ordered phase, which is a manifestation of the general tendency in the theory of cooperative phenomena of the effect of fluctuations on the results of the mean-field approximation. Theoretically, a similar calculation could be done for the case of antiferromagnetic instability, although the computation of sums over discrete frequencies is certain to be much more complicated. Let us return to b. Note that this quantity is proportional to the factor n_0 specified in (4.9), which for $T\ll\mu$ behaves like a unit step function:

$$n_0=\begin{cases}1, & \mu>0,\\ 0, & \mu<0.\end{cases} \qquad (6.22)$$

As shown in a detailed discussion in Refs. 3 and 4, the region $\mu<0$ corresponds to the collectivized-magnetism mode and the region $\mu>0$ to magnetism with localized magnetic moments. Thus, in the neighborhood of point $\mu=0$ there is a crossover from one mode to the other. The parameter b is finite only in the localized-magnetism region. Since it is this parameter that is responsible for the appearance of nonquasiparticle states, we can conclude that in a strongly correlated system with electron concentrations $n>n_c$, where n_c is the critical concentration at which $\mu=0$, the Fermi-liquid pattern is disrupted near magnetic phase transitions and the electronic states cease to be quasiparticle. The physical explanation for this is the scattering of electrons on quasistatic fluctuations of the order parameter, which near the transition point dominate over inelastic scattering processes. The latter do not change their qualitative behavior in the transition through point n_c. Superposed on the nonspecific action of inelastic scattering processes over a broad range of electron concentrations n (these are determined by the dynamic contributions to the magnetic susceptibility), the scattering on quasistatic fluctuations switches on abruptly for $n>n_c$ and therefore must be noticeable.

In conclusion we note that the validity of the approximate reduction of Eq. (6.1), an integral equation in momenta, to an algebraic equation has been analyzed by directly studying Eq. (6.1). Integration over the angle
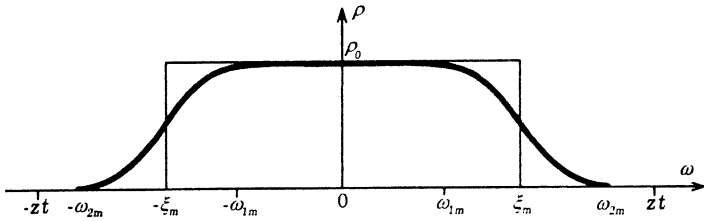
FIG. 8. Electronic-state density near a ferromagnetic phase transition (heavy curve). The light line represents the model density of states for electrons in the Hubbard-I approximation.

between vectors $\mathbf{k}$ and $\mathbf{k}_1$ yields the logarithmic term in the integrand, which gives rise to no poles in the Green's function. For this reason the procedure of taking the Green's function at the point of peak magnetic susceptibility outside the sum in Eq. (6.1) provides a good approximation to the solution of the initial equation, and the closer we are to a magnetic phase transition the better the approximation.

Now let us study the density of single-particle electronic states

$$\rho(\omega) = -\frac{1}{\pi}\sum_\sigma \frac{1}{N}\sum_\mathbf{k} \operatorname{Im} \mathscr{G}_\sigma(\mathbf{k};\omega). \qquad (6.23)$$

If we allow for Eq, (21), which links Δ with Σ for the paramagnetic phase, the expression (4.1) for the electron Green's function assumes the form

$$\mathscr{G}(\mathbf{k};\omega) = \frac{1}{\varepsilon(\mathbf{k})} \frac{\xi(\mathbf{k}) + \Sigma(\mathbf{k};\omega)}{\omega - \xi(\mathbf{k}) - \Sigma(\mathbf{k};\omega)}, \qquad (6.24)$$

from which we obtain the expression for the imaginary part of the Green's function:

$$\operatorname{Im} \mathscr{G}(\mathbf{k};\omega)$$

$$= \frac{\omega}{\varepsilon(\mathbf{k})} \frac{\operatorname{Im} \Sigma(\mathbf{k};\omega)}{[\omega - \xi(\mathbf{k}) - \operatorname{Re} \Sigma(\mathbf{k};\omega)]^2 + [\operatorname{Im} \Sigma(\mathbf{k};\omega)]^2}. \qquad (6.25)$$

Due to the specific form (6.24) of the function $\mathscr{G}$ ($\mathscr{G}$) $\times(\mathbf{k};\omega)$, its imaginary part acquires a weight factor $\omega/\varepsilon(\mathbf{k})$, by which the behavior of a strongly correlated system is distinguished from that of a Fermi liquid.

In the case of ferromagnetic instability, we must substitute the expression for Σ obtained from Eq. (6.3) into (6.25). After integrating with respect to $\varepsilon(\mathbf{k})$ in the expression (6.1) for the model of a constant density of states ρ_0, we arrive at the following:

$$\rho(\omega) = \rho_0, \quad |\omega| < \omega_{1m}, \quad \rho(\omega) = 0, \quad |\omega| > \omega_{2m};$$

$$\rho(\omega) = \rho_0 \left\{ \frac{1}{2} + \frac{1}{\pi}\arcsin\left(\frac{\xi_m - |\omega|}{\xi_m - \omega_{1m}}\right) \right.$$

$$\left. + \frac{1}{\pi}\frac{\xi_m - |\omega|}{(\xi_m - \omega_{1m})^2}\sqrt{(\omega_{2m} - |\omega|)(|\omega| - \omega_{1m})} \right\},$$

$$\omega_{1m} < |\omega| < \omega_{2m}. \qquad (6.26)$$

Here all the quantities with the subscript m represent the respective peak energies; for instance, $\varepsilon_m = tz$, $\xi_m = (1 - \frac{1}{2}n)tz$, etc. The width of the spectrum broadening

is $4\sqrt{b}\,tz$, that is, is determined by $\sqrt{b}$ (Fig. 8). Similar broadening in an interval of the order of $2btz$ occurs in the event of antiferromagnetic instability.

7. CONCLUSION

We have shown that in a strongly correlated system near a magnetic phase transition the electronic states are not of the quasiparticle nature due to the scattering of electron on quasistatic magnetic fluctuations. This is obvious from the analytical [Eq. (6.5)] and diagrammatic (Fig. 6) expressions for the Green's function in the case of ferromagnetic instability and the similar expressions in the case of antiferromagnetic instability. The parameter controlling the nonquasiparticle behavior is b. According to the definition (6.4), this quantity is actually the root mean square of the magnetic moment localized at a lattice site. What is remarkable is that a similar parameter appears in the self-consistent theory of spin fluctuations in an ordinary Fermi system;[7] it leads to a contribution of the Curie type to the magnetic susceptibility.

In the expression (6.5) for G (and in all the expressions that follow) there is a transition to the limit $b \to 0$ in the Hubbard-I approximation, and this corresponds to a quasiparticle description. The broadening of the delta function into a band for the spectral density of the function $G(\mathbf{k};\omega)$ is of a static nature rather than a dynamic (which usually leads to damping of the quasiparticle state), and in this sense resembles the nature of a quasilocal level in the impurity problem. The width of the band of incoherent states near the energy $\xi(\mathbf{k})$ is of order $\sqrt{b}$ for ferromagnetic instability and of the order of b for antiferromagnetic. To estimate the extent to which a state with a given momentum $\mathbf{k}$ is nonquasiparticle these quantities must be compared with the factor $1 - \frac{1}{2}n$. The parameter b is at its maximum at the phase transition point but evidently is small compared to unity.

The incoherent nature. of the electronic states in the Hubbard model in the situation of a half-filled band was discovered long ago. In Refs 19–21 it was found that near $n = 1$ (low hole concentration) in the region of antiferromagnetic ordering a hole becomes self-localized owing to the formation of a magnetic polaron, and, naturally, such nonpropagator states are described by an incoherent Green's function.

The mechanism for forming nonquasiparticle states studied here is, apparently, not the only one in a strongly correlated system. We considered effects of quasielastic

scattering of electrons on magnetic fluctuations near a magnetic phase transition. Similar effects must also manifest themselves near the dielectric instability of the system. Moreover, for some electron concentrations there obviously exist other mechanisms (operating far from the magnetically ordered phase) that disrupt the Fermi-liquid pattern. These, of course, are not easy to study by analytical methods because they are related to processes of inelastic scattering of electrons on fluctuations.

Another result is the study of magnetic phase transitions in the t–J model in the mean-field approximation. Using it we obtained equations for the order parameters in the ferromagnetic and antiferromagnetic phases for a broad range of electron concentrations. The equations reflect the dual nature of magnetism in a strongly correlated electron system, manifesting features of collectivized and localized magnetism simultaneously. What is remarkable is that the linearized equations for the order parameters lead to values of T_C and T_N coinciding with those found from the conditions for the divergence of the DC magnetic susceptibility of the paramagnetic phase. This indicates a second-order magnetic phase transition. The formulas for T_C and T_N illustrate the opposite nature of ferromagnetic and antiferromagnetic ordering in the t–J model: ferromagnetism is caused by the motion of electrons in the lattice and effective exchange only inhibits it, while antiferromagnetism emerges because of effective exchange and the motion of electrons inhibits it. In the situation of a half-filled band and fairly strong exchange interaction antiferromagnetism dominates in the system.

[1] P. W. Anderson, Science 235, 1196 (1987).

[2] Yu. A. Izyumov, Usp. Fiz. Nauk 161, No. 11, 1 (1991) [Sov. Phys. Usp. 34, 938 (1991)].

[3] Yu. A. Izyumov and B. M. Letfulov, J. Phys.: Condens. Matter 2, 8905 (1990).

[4] Yu. A. Izyumov and B. M. Letfulov, Int. J. Mod. Phys. B 6, 321 (1992).

[5] Yu. A. Izyumov, B. M. Letfulov, and E. V. Shipitsyn, J. Phys.: Condens. Matter 4, 9955 (1992).

[6] Yu. A. Izyumov, B. M. Letfulov, E. V. Shipitsyn, M. Bartkowiak, and K. A. Chao, Phys. Rev. B 46, 15 697 (1992).

[7] T. Moriya and A. Kawabata, J. Phys. Soc. Jpn. 34, 639 (1973).

[8] T. Moriya and H. Hasegawa, J. Phys. Soc. Jpn. 48, 1490 (1980).

[9] A. Kawabata, J. Phys. F 4, 1477 (1974).

[10] R. O. Zaĭtsev, Zh. Eksp. Teor. Fiz. 70, 1100 (1976) [Sov. Phys. JETP 43, 574 (1976)].

[11] J. Hubbard, Proc. Roy. Soc. London, Ser. A 276, 238 (1963).

[12] T. Izuyama, D. Kim, and R. Kubo, J. Phys. Soc. Jpn. 18, 1025 (1963).

[13] Yu. A. Izyumov and Yu. N. Skryabin, Statistical Mechanics of Magnetically Ordered Systems, Nauka, Moscow, 1987 [in Russian].

[14] A. A. Abrikosov, L. P. Gor'kov, and I. Ye. Dzyaloshinski, Quantum Field Theoretical Methods in Statistical Physics, Pergamon, New York, 1965.

[15] P. Coleman, Phys. Rev. B 29, 3035 (1984).

[16] D. M. Edwards and J. A. Hertz, J. Phys. F 3, 2174 (1973).

[17] R. O. Zaĭtsev, Zh. Eksp. Teor. Fiz. 75, 2362 (1978) [Sov. Phys. JETP 48, 1193 (1978)].

[18] A. O. Anokhin, V. Yu. Irkhin, and M. I. Katsnelson, J. Phys.: Condens. Matter 3, 1475 (1991).

[19] W. F. Brinkman and T. M. Rice, Phys. Rev. B 2, 1324 (1970).

[20] L. N. Bulaevskiĭ, E. L. Nagaev, and D. I. Khomskiĭ, Zh. Eksp. Teor. Fiz. 74, 1562 (1968) [Sov. Phys. JETP 27, 836 (1968)].

[21] E. Dagotto, R. Joynt, A. Moreo, S. Bacci, and E. Gagliano, Phys. Rev. B 41, 9049 (1990).

Translated by Eugene Yankovsky

This article was translated in Russia. It is reproduced here the way it was submitted by the translator, except for stylistic changes by the Translation Editor.